Iris Recognition Algorithm Optimized for Hardware Implementation

K. Grabowski, W. Sankowski, M. Napieralska, M. Zubert, A. Napieralski

Department of Microelectronics and Computer Science, Technical University of Lodz
al. Politechniki 11, 90-924 Lodz, Poland, {kgrabowski, wsan, mnapier, mariuszz, napier}@dmcs.pl

Abstract: **Iris recognition is accepted as one of the most efficient biometric method. Implementing this method to the practical system requires the special image preprocessing where the iris feature extraction plays a crucial role. Recognition is preceeded by iris localization which consists in finding the iris boundaries as well as eyelids. In this paper the short introduction into iris localization and wavelet-based iris identification method optimized for embedded systems is described. Proposed solution was applied to high resolution images taken under near infrared light.**

I. Introduction

Security of computer and financial systems plays crucial role nowadays. These systems require remembering many passwords that may be forgotten or even stolen. In the second case results are usually disastrous for the user. Thus biometrical systems, based on physiological characteristics of a person, are taken into consideration for growing number of applications. Moreover technical progress, along with civilization development, is associated with rising number of dangerous diseases, therefore touchless methods for user authentication, such as iris recognition, became a very attractive solution.

The first successful implementation of iris recognition system was proposed by J. Daugman in 1993 [5]. This work, though published more than 10 years ago, still remains very valuable because it presents well thought solutions for each part of the system. His publication is known as fundamental in the area of iris identification and further researchers refer to it. It is worth mentioning that most available operational iris recognition systems worldwide today are based on the algorithms described by J. Daugman [5]. However new promissing methods for iris feature extraction have been developed based on 2D wavelet decomposition [2]. Because of using simple wavelets in mentioned analysis, this method can be implemented in a hardware platform.

II. Localization

It should be underlined that all considerations in this paper refer to high resolution images taken directly from a camera under Near Infrared light (NIR) without preprocessing. The image zooms in eye only. In this section a novel approach to iris segmentation is presented, its preliminary results are described in more detail in [1].

The first step in the localization process is pupil segmentation based on analysis of the histogram. It is assumed, like in [8], that a pupil is the darkest area in the image and standard deviation of luminance in this area is relatively low. It has to be emphasized that unwanted elements (reflections, eyelashes, etc) may appear in the thresholded image. Nevertheless pupil can be segmented by relatively simple method, based on image thresholding using the histogram analysis. It is possible, because in general, histogram function of all NIR eye images have a local maximum placed in the area of small luminance values (pupil).

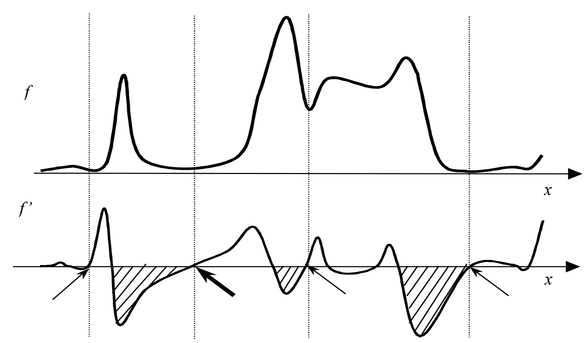

Fig. 1. Example of typical NIR eye image histogram f and its derivative f'- where x is a luminance. Bolded arrow shows desired point of segmentation.

The point of segmentation, which is marked in figure 1 by bolded arrow, is computed with operator (1) described in details in [1].

$$P_{(p)} : \left\{ \underset{x \mapsto f'(x) \le 0}{\forall} \frac{1}{L} \sum_{i=x_0}^{p=x_0+L} f'(i) \right\} \quad (1)$$

where: x_0 – zero-cross point of histogram function *f(i)*, *L* – distance to next zero crosspoint towards growing intensity values *i,P* – set of potential thresholds from which the smallest element *p* is chosen.

The operator (1) searches for significant falling edges of the histogram function, and points to a first significant local

1-4244-0623-4/06/$20.00 ©2006 IEEE.

minimum. The operator uses smoothed derivative of the histogram function and for rounding first order polynomial is used. Since the first local maximum represents pupil for this kind of images, the presented method causes that pupil is always thresholded. Obviously reliability of the pupil segmentation method strongly depends on histogram function shape, but it was verified [1] that the local maximum is common for histograms of images with assumed framing and illumination.

This approach has an advantage in relatively low algorithm complexity due to vectorial arithmetic representation.

When pupil segmentation using found threshold is completed, next operation is required for removing reflections and other unwanted elements. It is essential for the next steps of the algorithm. The following morphological operations are used for artifacts removing:

- morphological opening for clearing out small elements which are present in thresholded image (i.e. eyelashes, eye makeup and others);
- morphological closing for removing reflections from pupil area (if present);

In both cases a circle as a structuring element is used, however its size differs for opening and closing operations. As a result the binary image with quasiround and homogenous pupil area is obtained (in most cases without other elements). Then “black hole search method” is applied for pupil positioning and quasiradius assignation, described in [1, 8]. Using mass center method ensures that even noncircle form will be well centered. This is necessary because the pupil may be slightly misshaped depending on various conditions (light, eye tiredness, etc). Since the pupil has a round shape a quasi-radius with formula presented in [1,8] is calculated.

Daugman’s integral differential operator is applied for outer border [5]. The angle limitation to 90° for both sides asserts high probability that neither upper nor lower eyelid will cause an error when luminance gradient is being determined. Assuming that pupil and iris are non concentric, the search for iris center is performed independently. Iris center is searched in the area around pupil center which has been found in previous steps. The chosen rectangle is placed at the center of a pupil. Its width to height ratio is about 11:3 and its size is proportional to the image and pupil size ratios in pixels. This saves a lot of computing power in case of implementation in embedded systems. This assumption is possible because the pupil-iris center displacement statistically does not exceed relatively small range.

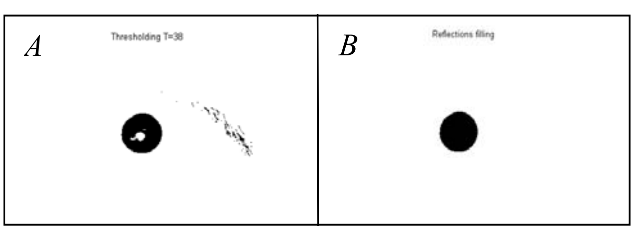

Fig. 2. A – result of segmentation, B – result of clearing and filling operation

Exemplary results of pupil segmentation are depicted in figure 2A. The presence of segmented eyelashes and pupil holes caused by light reflection is observed.

In figure 2B result of morphological operations is presented. Operations used for pupil segmentation and morphological clearing are easy to achieve in fixed-point environment, therefore can be implemented e.g. in FPGA.

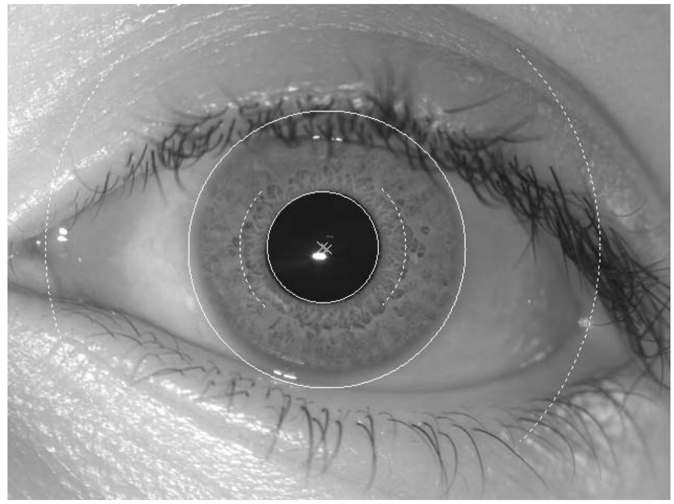

Fig. 3. Result of pupil and iris localization. Dashed arcs show range of search byDaugman’s operator, cross symbols show centers of pupil and iris, circles outline computed inner and outer borders respectively.

Result of the whole localization process is presented in figure 3. Coordinates of centers, radiuses of iris and pupil are the output arguments of proposed localization algorithm.

The next step is iris enrollment. After successful pupil and iris localization (center coordinates and radiuses) an extraction of iris image is performed with formula given and explained in [5]:

$$\begin{aligned} x(r,\theta) &= (1-r)x_p(\theta) + r x_s(\theta) \\ y(r,\theta) &= (1-r)y_p(\theta) + r y_s(\theta) \end{aligned} \tag{2}$$

This transformation allows remapping iris image $I(x,y)$ from raw coordinates (x,y) to the doubly dimensionless non concentric polar coordinate system $I(r,\Theta)$, where points (x_p, y_p) and (x_s, y_s) are placed in the given angle on pupil and iris border respectively.

In order to obtain multiresolution iris images, additional Gauss interpolation was applied. As it turned out experimentally the pixel interpolation is not required for high resolution images when wavelets decomposition for feature extraction is further applied.

The histogram of extracted and enrolled iris has to be equalized in order to increase contrast. Results of these operations are presented in figure 4.

A reliability of proposed localization algorithm was estimated at 96% for University of Bath Iris DB, which contains original, high resolution eye area pictures, taken under NearIR illumination. It is worth mentioning that any displacement between algorithm result and real center of the pupil is considered as an error.

Pupil's segmentation errors are caused in principle by light reflections placed near pupil-iris border. It results in displacing mass center to false coordinates and further in incorrect iris extraction. But these can be avoided by system design where illumination is properly placed.

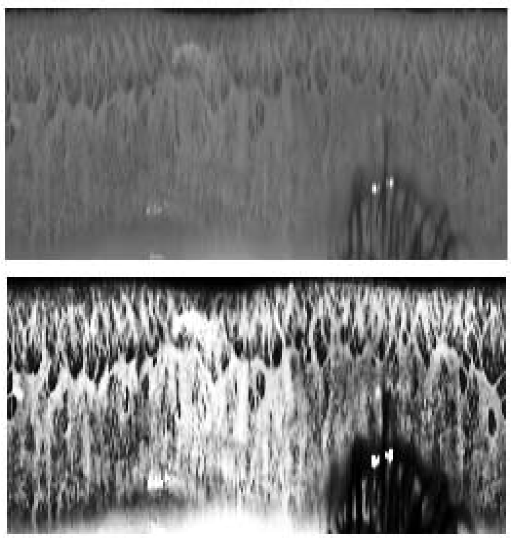
A
B

Fig. 4. Extracted iris from image presented in figure 3. A-original enrolled iris, B-enrolled iris after histogram equalization.

Presented method cannot be used for images with bigger framed area, i.e. face where other dark areas may be present (CASIA v.2) for similar reasons. Because of using operator (1) for image segmentation the method can be used only for the continuous histogram functions, thus it does not work properly with preprocessed databases like e.g. MMU.

III. Features extraction identification

Most of iris recognition systems are based on Gabor wavelet analysis in order to extract iris image features. This method was proposed by Daugman in [5]. It consists in convolution of image with complex Gabor filters. As a product of this operation, phasors (complex coefficients) are computed. In order to obtain iris signature, phasors are evaluated and coded by their location in the complex plane. However the Daugman's method is patented which blocks its further development.

Very attractive solution was proposed by ISEP Iris research team in [2, 3]. This solution uses 2D Discrete Wavelet Transform (DWT) for features extraction. Results of identification algorithm using DWT for several kinds of wavelets: Haar, Daubechies, biorthogonal, coiflets and symlets [2] were obtained. In this paper Haar and Biorthogonal wavelets were determined as the most suitable for identification. Especially the first one is interesting because it can be easily implemented e.g. in fixed-point environment. In this case, features can be understood as coefficients of wavelet transform. Important issue for such kind of analysis is on what decomposition level and which packet (approximation or detail HVD) contained information is significant.

For this purpose special operator (3) was used to estimate global energy:

$$E_i = \sum_{j,k} w_i(j,k)^2 \quad (3)$$

where: j,k – coordinates, i – packet number.

It has to be emphasized that in order to make proper coefficients more significant, iris image is enhanced by increasing contrast – see figure 4. This is necessary when discrete wavelet transform is performed, because image convolution with e.g. Haar wavelet will produce more significant coefficient when high luminance change will occur in a given coordinates – e.g. "hill" to "hollow" transition in iris pattern.

Enrolled iris image is decomposed into 4 parts: approximation, horizontal, vertical and diagonal details (AHVD) and from each of these parts next decomposition is performed. Third level of decomposition is achieved and 64 subimages are ready for their energy measurement. As a result of this method 2 subimages (packets) are identified where information energy is significant: packet number 2 and 10. Details of this measurment are presented in [2].

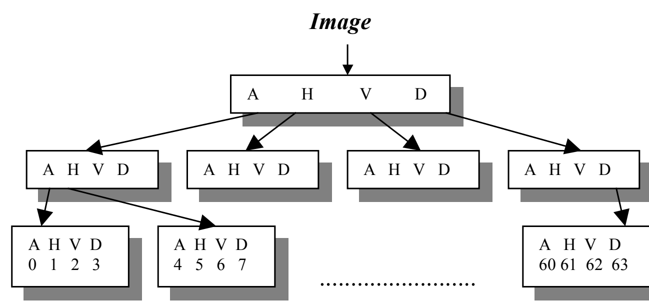

Fig. 5.Iris image decomposition tree

In order to obtain iris code, the following method of discrimination is used:

$$\begin{aligned} c_{i,j} &= 0 & \left|w_{i,j}\right| &< T \\ c_{i,j} &= 1 & w_{i,j} &\geq T \\ c_{i,j} &= -1 & w_{i,j} &\leq T \end{aligned} \quad (4)$$

coefficients are compared to value T, experimentally estimated at $T=10$ and after this operation 3 possible values for one element are obtained. Therefore, applying this method, we can calculate the number of possible iris codes (5).

$$PossibleIrisCodes = 3^{\left(\frac{x \cdot y}{8}\right)} \quad (5)$$

where: x,y – resolution of enrolled iris image, 8 – degree of input image decomposition at level 3 – for DWT input image is downsampled by $2^3=8$.

In our research, differently than in [2, 3], we use enrolled iris images with size 256x128 pixels, which finally gives $1{,}93 \cdot 10^{244}$ possible iris codes.

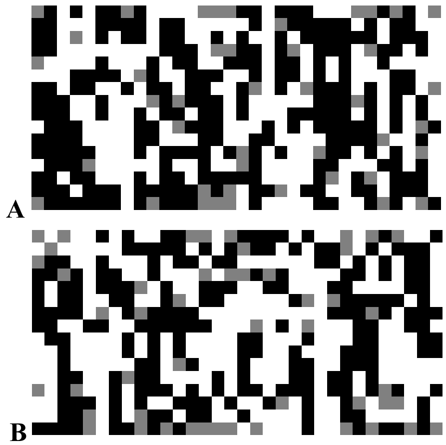

Fig. 6. Iris signatures of subimages 2 and 10 taken from iris pattern - figure 4B

Example of graphical representation of iris code is presented in figure 4.

Discrete Wavelet Transform can be easily implemented in reprogrammable or DSP environment because it can be achieved by simple operations like high-pass and low-pass filtering and downsampling [6, 7]. Two dimensional discrete wavelet transform graph is depicted in figure 7.

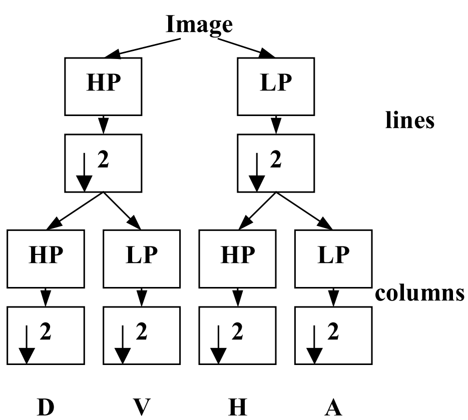

Fig. 7.Discrete Wavelet Transform realization using filtering and downsampling.

IV. Identification

Identification of two iris codes is the final operation of the algorithm. The most common comparison method of iris signatures for researchers in this area is Hamming Distance (HD). However HD has to be slightly modified in order to adapt to 3 degrees of freedom of one element in iris code and also it has to take into account 2 codes from one iris (packet 2 and 10 are considered as independent signature). In our case HD is given by formula (6).

The decision whether two iris codes match or differ is based on the certain value of HD. This threshold is called Decision Value (DV) which was estimated in [2, 3] at approx. 0.34.

$$HD^{(2)} = \frac{\sum_i \sum_j \left| c_1^{(2)}(i,j) - c_2^{(2)}(i,j) \right|}{2 \cdot i \cdot j}$$

$$HD^{(10)} = \frac{\sum_i \sum_j \left| c_1^{(10)}(i,j) - c_2^{(10)}(i,j) \right|}{2 \cdot i \cdot j} \qquad (6)$$

$$HD = 2 \cdot HD^{(2)} \cdot HD^{(10)}$$

where: $HD^{(2)}$, $HD^{(10)}$ – Hamming Distances of iris codes extracted from packet 2 and 10 respectively.

Hamming Distance computed from two irises below DV means that irises belong to the same person otherwise irises are recognized as different.

V. Experimental results

It has to be stated that images in iris image database used in [2, 3] do not have any occlusions like eyelids or eyelashes inside iris area. Thus no disturbances in iris pattern are present – eyes are widely open and whole iris is clearly visible. In practice such situation will seldom occur, because it is imposible to obtain such perfect image every time in real system. Therefore, in our research we decided to check the influence of averaging effects, which are inseparable part of wavelet analysis, on Hamming Distance when eyelashes are present in the iris background. It is worth mentioning that there are methods for removing occlusions but elimination of eyelashes cannot be guaranteed.

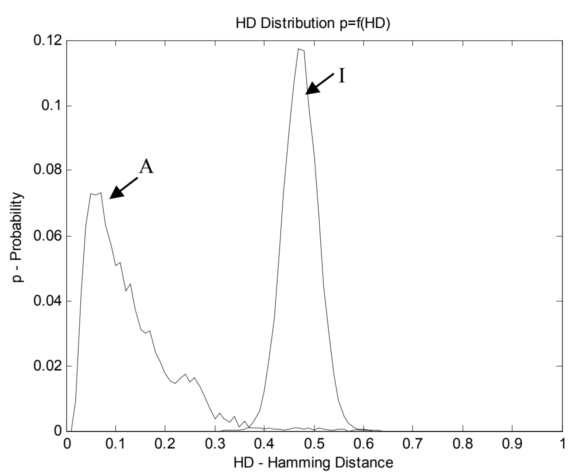

Fig. 7. Hamming distance distribution for "authentics" (A) and " imposters" (I).

In order to estimate distribution of Hamming Distance scanning of 1000 eye pictures from University of Bath Iris DataBase was performed. The database contains 20 pictures of both eyes for 50 persons. The initial results of mentioned analysis are depicted in figure 7.

Natural iris images were used for analysis; no operation for removing artifacts (occlusions or eyelids) was done. As it can be noticed in figure 7, in case of high resolution pictures taken under NIR light, “imposters” HD distribution do not exceed specified range: 0.32 ÷ 0.62 and has a gaussian shape. Thus it can be assumed that Decision Value in this case equals 0.32. Left offset, in reference Hamming Distance equal to 0.5, can be caused by artifacts. For databases where whole iris is visible the Decision Value for presented wavelet feature extraction method was estimated at 0.34 in [2, 3] on the basis of HD distribution of authentics and imposters, simiralrly to figure 7.

The influence of occlusions and eyelashes is observed in “authentics” distribution. Significant number of “authentics” comparisons gives “imposter” result when Decision Value e.g 0.32 is assumed. Mentioned value is not general, but was estimated by statistical analysis for specified database (Bath). In order to estimate general DV (for given feature extraction method) more experiments and analysis should be done.

Summarizing, none “imposter” will be found as “authentic” for e.g 0.32 Decision Value even when no artifacts removing operation is performed.

VI. Summary and future work

Presented algorithm had been tested on University of Bath Iris Image Database [9] which contains 2000 images, in high 1280x960 resolution and 8-bit luminance depth. The undertaken work is focused on images obtained directly from a camera under NIR light illumination without any image processing. The proposed localization method gives 100% efficiency for CASIA v.1 [10], HD distribution for this database has not been performed yet.

Features extraction based on wavelet packets was found as satisfactory method for iris comparison with relatively high trust rate. In the future, we plan to implement presented algorithm or its part into FPGA chip, built-in frame-grabber device. Camera and optical system will ensure that desired eye area will be framed in an image so it will be possible to use localization methods presented in this paper.

VII. Acknowledges

The work reported in this paper was supported in part by the Polish State Committee for Scientific Research Grant 3 T11 B00 827 and Internal University Grant K-25/1/2006-Dz.S. The authors acknowledge University of Bath to make their Iris Image Database available to our Department and The Center for Biometrics and Security Research (CBSR) – Chinese Academy of Sciences – for their CASIA Database.

A special acknowledge is due to Iris Research team from Institute Superieur d’Electronique de Paris (ISEP), France for cooperation.

References

[1] K. Grabowski, W. Sankowski, M. Zubert and M. Napieralska, “Reliable Iris Localization Method with Application to Iris Recognition in Near Infrared Light”, *International Conference Mixed Design of Integrated Circuit and Systems* – MIXDES’06, Gdynia Poland, June 22-24, 2006

[2] F. Rossant, M. T. Eslava, T. Ea, F. Amiel and A. Amara, “Iris Identification and Robustness Evaluation of a Wavelet Packets Based Algorithm”, *IEEE International Conference on Image Processing* – ICIP '05, Genova, September 11-14, 2005

[3] E. Rydgren, T. Ea, F. Amiel, F. Rossant and A. Amara “Iris Features Extraction Using Wavelet Packets”, *IEEE International Conference on Image Processing* – ICIP '04, Vol. 2, pp. 861-864, Singapore, October 24-27, 2004

[4] J. Daugman, “The Importance of Being Random: Statistical Principles of Iris Recognition”, *Pattern Recognition*, vol. 36, no. 2, pp. 279-291, Madison Wisconsin, June 16-22, 2003

[5] J. Daugman, "High Confidence Visual Recognition of Persons by a Test of Statistical Independence", *Trans. Pattern Analysis and Machine Intelligence*, Vol.15, No 11, pp. 1148-1161, 1993

[6] T. Ea, A. Valentian, F. Amiel, F. Rossant and A. Amara “Implementation on SoPC of Algorithms Dedicated to Iris Identification” – private communication

[7] T. Ea, A. Valentian, F. Amiel, F. Rossant and A. Amara “Algorithm implementation for IRIS identification”, *48th Midwest Symposium Circuits and Systems,* pp. 1207- 1210, August 7-10, 2005

[8] C. Teo and H. Ewe, "An Efficient One-Dimensional Fractal Analysis for Iris Recognition", Proceedings of the *13-th WSCG International Conference in Central Europe on Computer Graphics*, Visualization and Computer Vision, pp. 157-160, Plzen-Bory, Czech Republic, January 31 – February 4, 2005

[9] University of Bath Iris Image Database, URL:http://www.bath.ac.uk/ elec-eng/pages/sipg/irisweb/database.htm#

[10] CASIA Iris DataBase, URL: http://www.sinobiometrics.com